

Second-order fluorimetric approach based on a boron dipyrromethene (BODIPY) tetraamide derivative for Hg(II) chemosensing in water and fish samples

Valeria A. Lozano,^a Arsenio Muñoz de la Peña,^{b,*} Graciela M. Escandar^{a,*}

^a *Instituto de Química Rosario (CONICET–UNR), Facultad de Ciencias Bioquímicas y Farmacéuticas, Universidad Nacional de Rosario, Suipacha 531 (2000) Rosario, Argentina.*

^b *Department of Analytical Chemistry, University of Extremadura, 06006, Badajoz, España.*

* Corresponding authors. Tel/fax: 0054-341-4372704 (G. Escandar), E-mail addresses: arsenio@unex.es (A. Muñoz de la Peña), escandar@iquir-conicet.gov.ar (G. Escandar)

A new fluorimetric method is described for the determination of Hg(II), based on the selectivity of a boron dipyrromethene tetraamide derivative (BODIPYTD) towards this ion, in combination with second-order chemometric analysis, to deal with matrix interferences. This is the first time that the selectivity of a mercury chemosensor regarding other metal ions is reinforced with the selectivity offered by second-order calibration, which is able to overcome the potential interference produced by organic constituents of natural or bio-samples. After the BODIPYTD-Hg(II) complex was formed, the excitation-emission fluorescence matrix was recorded and parallel factor analysis (PARAFAC) was applied for data processing. This algorithm achieves the second-order advantage and was able to overcome the problem of the presence of unexpected interferences. The method was applied to the direct determination of Hg(II) ion in environmental waters and fish muscle tissues, with minimal pretreatment steps and without the need of organic solvents. The results were successfully evaluated through a spiking recovery study in both types of real samples, which have constituents displaying fluorescence signals potentially able to interfere in the analysis. This latter fact demonstrates the excellent selectivity of the proposed method. The studied concentration range in water samples was 10-30 ng mL⁻¹, while in fish samples it was 0.12-0.30 µg g⁻¹. The limits of detection for water and fish samples were 2 ng mL⁻¹ and 4×10⁻³ µg g⁻¹, respectively, with relative prediction errors below 5%, and a sample throughput of about 8 samples per hour.

Introduction

Because of its high toxicity and stability in the aquatic environment, Hg(II) is considered as a priority pollutant.¹ This metal ion can be transformed via biotic and/or abiotic methylation into methyl mercury, a potent neurotoxin that concentrates through the food chain in the tissue of fishes. Subsequent ingestion by humans of seafood contaminated with this mercury derivative can cause adverse effects in vital organs and tissues, such as liver, brain and heart muscle.² Therefore, the concern of regulatory agencies to control the presence of Hg(II) and its derivatives in environmental samples is not surprising.³

Current analytical methods for mercury screening, including cold vapor atomic absorption spectroscopy⁴ and inductively coupled plasma-mass spectrometry⁵ require sophisticated and expensive equipment and frequently sample pre-processing steps. In the last decade, substantial efforts have been focused towards the development of fluorescent chemosensors and chemodosimeters for sensitive and selective routine monitoring of mercury in water and biological samples. Rhodamine⁶⁻¹² and 4,4-difluoro-4-bora-3a,4a-diaza-s-indacene or difluoroborondipyrromethene (BODIPY)¹³⁻¹⁸ derivatives are two of the most employed families of chemosensors for mercury detection. Culzoni et al. have reviewed both rhodamine and BODIPY-based fluorimetric sensors for Hg(II) ion, as applied to environmental and biochemical samples such as mineral, underground, river, pool, tap, lake and sea water samples, living cells, and fish samples.¹⁹ In this latter review, the structures of the numerous synthetic derivatives used as mercury sensors and their recognition mechanisms are discussed.

Specifically, BODIPY derivatives have several outstanding features, including high fluorescence quantum yield and fine tunable spectroscopic properties.²⁰ Recently, a chemosensor based on a BODIPY derivative armed with a tetraamide receptor (BODIPYTD, see Fig. 1) was described for the fluorimetric determination of Hg(II) in environmental water samples.¹⁸ While this particular derivative exhibits a weak fluorescence emission intensity due to a deactivating photo–electron transfer (PET) effect acting over the BODIPY core, an intense fluorescence signal is detected in the presence of Hg(II). This increase in emission intensity was assigned to mercury complex formation involving the nitrogen atoms of the receptor moiety, which blocks the deactivating PET mechanism.¹⁸ Consequently, the system displays an intense OFF-ON fluorescence enhancement, allowing the metal ion determination at very low concentrations.

It was demonstrated that the fluorescence of this chemosensor, highly selective towards Hg(II) ion, is not significantly affected by other competing metal ions such as Li(I), Na(I), K(I), Ag(I), Mg(II), Ca(II), Ba(II), Fe(II), Fe(III), Cu(II), Zn(II), Cd(II), Co(II), Pb(II), and Al(III), and successful Hg(II) recoveries were obtained in spiked tap and waste water samples.¹⁸ However, it is likely that real environmental and biochemical matrices will contain other fluorescent constituents (organic pollutants, humic and fulvic acids, waste materials, degradation products, pharmaceuticals and their metabolites, aminoacids, proteins, etc.) which could interfere in this spectrofluorimetric determination, for example by displaying overlapping spectra. In fact, the determination of contaminants in complex samples usually faces the problem of the presence of interfering agents, which must be removed before quantification, extending the analysis time and the experimental work. In addition, these separation

steps frequently involve the use of significant amounts of toxic organic solvents, in disagreement with the green analytical chemistry principles.²¹

Therefore, a second-order multivariate calibration protocol using the presently discussed BODIPYTD chemosensor is proposed in this work, as a useful approach for the determination of Hg(II) ion in the presence of any expected or unexpected potential interferences, with overlapping fluorescence excitation and/or emission spectra. Second-order calibration allows reaching the second-order advantage,²² which refers to the capacity of certain algorithms of allowing the accurate prediction of analyte concentrations in complex samples containing potential interferences.²³ This useful property avoids the requirement of interference removal, with the concomitant saving of experimental work, analysis time, and use of toxic organic solvents required by clean-up procedures.

Specifically, the algorithm known as parallel factor analysis (PARAFAC)²⁴ was applied to the trilinear three-way data built with the excitation-emission fluorescence matrices (EEFMs) generated by the BODIPYTD-Hg(II) complex under optimal working conditions, and in the presence of other compounds selected as potential interferences. The fitting of a trilinear three-way array to the PARAFAC model often provides unique solutions, and the uniqueness of the decomposition is the natural basis of the PARAFAC second-order advantage. The latter is the main advantage offered by second-order calibration in comparison with the first-order counterpart.²²

It is interesting to note that this is the first time that second-order multivariate calibration is applied in combination with a chemosensing system. A comparison with other recently proposed schemes for Hg(II) detection is performed, and the feasibility of determining Hg(II) ion in real environmental and biological matrices is demonstrated by

applying the proposed methodology to river and underground waters, and to fish muscle tissues.

Experimental

Reagents and solutions

The synthesis of BODIPYTD (Fig. 1) and the confirmation of its structure by ^1H NMR and ^{13}C NMR were performed as indicated in ref. 18. $\text{Hg}(\text{NO}_3)_2 \cdot \text{H}_2\text{O}$, methanol, nitric acid and phosphate buffer were purchased from Merck (Darmstadt, Germany). Riboflavin, erythrosine and acridine were of analytical grade and were used as received.

A stock solution of BODIPYTD ($1.50 \times 10^{-4} \text{ mol L}^{-1}$) was prepared in methanol, and more diluted water solutions ($2.00 \times 10^{-5} \text{ mol L}^{-1}$) were prepared daily, taking an appropriate volume from this methanol solution, evaporating the solvent with N_2 to dryness, and diluting to the final volume with ultrapure water. The latter was obtained from a Millipore Milli-Q system (Millipore, Bedford, MA).

A $\text{Hg}(\text{II})$ stock solution ($1.50 \times 10^{-3} \text{ mol L}^{-1}$) was prepared by dissolving mercury(II) nitrate in doubly deionized water containing a few drops of concentrated HNO_3 . More dilute sample solutions were prepared daily by appropriate dilution of the stock solution with ultrapure water. A 0.5 mol L^{-1} phosphate buffer of $\text{pH}=7.50$ was also prepared.

All stock solutions were stored in amber glass bottles at $4 \text{ }^\circ\text{C}$. Special care was taken in the preparation and handling of solutions and containers to minimize any possible risk of mercury contamination. Calibrated flasks were left overnight in 10% (v/v) HNO_3 and rinsed with ultrapure Milli-Q water to eliminate contamination before use.

Instrumentation

Fluorescence measurements were performed on a Varian Cary Eclipse (Varian, Mulgrave, Australia) luminescence spectrometer equipped with a 7 W Xenon pulse lamp and connected to a PC microcomputer. The data matrices were collected at excitation wavelengths from 470 to 510 nm each 2 nm, and emission wavelengths from 520 to 570 nm each 1 nm. Both excitation and emission slit widths were of 5 nm. The photomultiplier tube sensitivity was set at 800 V, and the scan rate was 600 nm min⁻¹. All measurements were carried out using a 1.00 cm quartz cell, thermostated at 18.0 ± 0.1 °C by means of an RM 6 LAUDA thermostatic bath.

Procedure

A calibration set of six samples were prepared by triplicate in the concentration range 0–100.0 ng mL⁻¹ by adding appropriate amounts of Hg(II) ion stock solution and 50.0 µL of 2.00×10⁻⁵ mol L⁻¹ BODIPYTD water solution into 2.00 mL volumetric flasks. After stirring for 5 minutes in the darkness, each solution was diluted to the mark with phosphate buffer (0.5 mol L⁻¹, pH=7.50), and the EEFM was collected and subjected to second-order data analysis. The time elapsed between consecutive measurements (including the stirring step and the fluorescence matrix measurement) was about 7.5 min. A validation set was similarly prepared, employing Hg(II) concentrations different than those used for calibration and following a random design, i.e., with concentrations taken at random from the corresponding calibration range.

As will be demonstrated below, the compounds riboflavin, erythrosine and acridine, chosen as model of potential contaminants, display fluorescence signals which significantly overlap with that for the studied Hg complex. Therefore, with the purpose of evaluating the proposed strategy in an interfering environment, twelve additional test

samples containing random concentrations of Hg(II) ion and the above mentioned three compounds were prepared. The concentrations of the interfering agents in these latter samples were in the ranges 50.0–200.0 ng mL⁻¹ for riboflavin and erythrosine, and 250.0–500.0 ng mL⁻¹ for acridine.

Real samples

Because all samples (waters and fishes) did not contain Hg(II) ion at levels higher than the attained detection limit, a recovery study was carried out by spiking them with the metal ion at different concentrations.

Water samples

A river water sample (Paraná River, Argentina) was collected near a region of high industrial activity, and underground water samples were obtained from two different cities (Venado Tuerto City and Santa Rosa City, Argentina) located at about 400 km away from each other. In order to remove suspended solid materials, the evaluated river and underground water samples were filtered through filter paper and through a nylon membrane. To mimic a real situation, filtration was performed after the addition of the Hg(II) standard solution. BODIPYTD aqueous solution was then added, and samples were subjected, by duplicate, to the same procedure employed for the validation ones.

Fish samples

Fishes (tuna and mackerel) were collected from commercial markets. Three different fish samples were tested: two tuna and one mackerel sample. A portion of the muscle tissue was dried in an oven at 80 °C for 60 minutes. After grinding the dry tissue, 0.2000 g of each sample was weighed, spiked with the analyte, and digested in nitric acid at

100 °C for 100 minutes. The mixture was filtered with a paper disk into a volumetric flask and diluted with phosphate buffer (0.5 mol L⁻¹, pH=7.50). The solution was then filtered through a C18 membrane, BODIPYTD aqueous solution was added, and the procedure described above was carried out. Each measurement was performed in duplicate. It is necessary to point out that acid digestion is applied, and thus the organic mercury species (e.g., methylmercury), if present, would render inorganic mercury, which adds to the original Hg(II) ion contained in the sample. Therefore, the total mercury content is determined following the proposed methodology.

Software

The theory of PARAFAC is well documented in the literature, and hence a brief description is supplied in the Supplementary Data. The employed chemometric algorithm (PARAFAC) was implemented in MATLAB 7.6,²⁵ using the codes provided by Bro²⁶ and the MVC2 graphical interface,²⁷ which can be freely downloaded from www.iquir-conicet.gov.ar/descargas/mvc2.rar. It is important to remark that analytical readers not familiarized with chemometric analysis may find thorough explanations about the MVC2 toolbox and the presently employed algorithm, including easily understandable examples, in a recently published book.²⁸

Results and discussion

Preliminary studies

Exploratory experiments confirmed that the optimal conditions to obtain the best signal were those indicated in a recent report.¹⁸ In fact, maximum fluorescence is observed when the BODIPYTD and Hg²⁺ react in a 1:2 ratio under stirring for five minutes in the

darkness, and then phosphate buffer (pH=7.50) is added in order to stabilize the fluorescence response of the complex.

Figure 2A shows the fluorescence excitation and emission spectra of BODIPYTD in the absence and in the presence of increasing concentrations of Hg(II) ion. As can be seen, the fluorescence signal increases with increasing concentrations of the analyzed ion, and a slight shift to the red of the emission band (ca. 5 nm) is also detected.

Quantitative second-order analysis

Synthetic samples

On the basis of the optimal conditions confirmed above, the spectrofluorimetric determination of Hg(II) ion using the BODIPYTD chemosensor was carried out. As previously demonstrated, the quantitation of the metal ion in matrices without organic interferences was successfully performed through a direct univariate or zeroth-order calibration.¹⁸ However, taking into account that environmental matrices may contain interfering constituents, a second-order chemometric analysis was proposed. Although the differences between excitation and emission spectra for free BODIPYTD and for the mercury complex are not significant (Fig. 2B), the employed second-order algorithm PARAFAC was able to distinguish these signals, rendering excellent results (see below). Figure 2B shows the normalized excitation and emission fluorescence spectra for free BODIPYTD in the absence and presence of Hg²⁺, and Fig. 2C displays the corresponding results in the presence of riboflavin, erythrosine and acridine. Notice that the profiles shown in Fig. 2B and 2C are normalized to unit length and do not represent true intensities.

Initially, under the optimal working conditions, EEFMs were recorded for calibration and validation samples, in the absence of additional compounds. Figure 3A shows the three-dimensional plot and the corresponding contour plot for the EEFM of a typical validation sample in the analyzed wavelength ranges.

PARAFAC was applied to three-way data arrays built by joining the calibration data matrices with those for each of the validation samples in turn. The algorithm was initialized with the loadings giving the best fit after a small number of trial runs, selected from the comparison of the results provided by generalized rank annihilation and several random loadings.²⁹ The number of components was selected by core consistency analysis,³⁰ and also through visual inspection of the spectral profiles produced by the addition of new components. If this addition generates repeated profiles, suggesting overfitting, this new component was discarded. The number of responsive components obtained in validation samples using both procedures was two, justified by the presence of two different signals: those arising from the BODIPYTD-Hg²⁺ complex and from free BODIPYTD. No restrictions were applied during PARAFAC least-squares fit.

Figure 4A shows the prediction results after the application of PARAFAC to the complete set of validation samples. As can be appreciated, the predictions for Hg(II) concentrations are in good agreement with the nominal values. With the purpose of assessing the accuracy of the predicted concentrations, the elliptical joint confidence region (EJCR) test was performed.³¹ The EJCR test consists of plotting, in the slope-intercept plane, the region of mutual confidence (usually at 95% confidence level) of the slope and intercept for the regression of predicted vs. nominal concentrations. The region has an elliptical shape, and the test consists in checking whether the theoretically expected values of slope = 1 and intercept = 0 are included within the ellipse. When the

ideal point is included within the EJCR, this indicates accuracy of the used methodology. Further details on the EJCR test can be found in the relevant literature.³¹ In the present case the ideal (1,0) point lies inside the EJCR surface (Fig. 4C), suggesting that PARAFAC is appropriate for resolving the system under investigation. The corresponding statistical results shown in Table 1 are also indicative of high-quality predictions. The limit of detection (LOD) was estimated with the approach described in ref. 32 according to the expression:

$$\text{LOD} = 3.3 \sqrt{hs_C^2 + hs_X^2 / \text{SEN}^2 + s_X^2 / \text{SEN}^2} \quad (4)$$

where h is the sample leverage at zero analyte concentration, s_C^2 is the variance in calibration concentrations, s_X^2 is the variance in the instrumental signal, SEN is the component sensitivity, and the factor 3.3 is the sum of t -coefficients accounting for types I and II errors (false detects and false non-detects, respectively) at 95 % confidence level.³² Equation (4) takes into account the propagation of all possible error sources (instrumental signal of the test sample, instrumental signal of calibration samples, and calibration concentrations) to the predicted concentration error.³²

The obtained limit of detection (LOD = 2 ng mL⁻¹) is significantly lower than that obtained using the same BODIPYTD chemosensor, but applying univariate calibration (LOD = 5.5 ng mL⁻¹, ref. 18), and this is a clear demonstration of the positive effect of the multivariate calibration on the sensitivity of the analysis.²³ The relative error of prediction (REP = 3 %) indicates a very good precision.

Because the real challenge is to obtain satisfactory predictions in systems where other foreign compounds are also present, fluorescent compounds which may interfere with the analysis were introduced in the test samples for evaluation. We found that the excitation and emission spectra of certain compounds commonly found in natural

waters such as riboflavin, erythrosine and acridine are significantly overlapped with those corresponding to the BODIPYTD-Hg²⁺ complex, producing a severe spectral interference (Figs. 2C and 3B). Riboflavin (vitamin B2) is a well-known pigment present in the waters of rivers, lakes and seas, which facilitates the photochemical transformation of many pollutants in the environment,³³ erythrosine is a synthetic dye used as a food additive frequently found in water as environmental pollutant,³⁴ and acridine is often detected in natural waters because several dyes and drugs contain the acridine skeleton. In fact, acridine is the major photodegradation intermediate of carbamazepine which, in turn, is one of the most frequently found emerging pharmaceutical contaminants.³⁵

In order to simulate a very unfavorable situation, the interferences were added at high relative concentrations with respect to Hg(II). The number of responsible components in these samples, selected by following a similar procedure to that indicated above for the validation samples, was three. These PARAFAC components were assigned to: (1) the mercury complex, (2) free BODIPYTD and (3) a combined signal corresponding to the interferences. Apparently, PARAFAC is not able to discern between the profiles of each individual foreign compound, and retrieves the interfering profile as a single unexpected mathematical component. However, this fact does not preclude the obtainment of good analytical results in these complex samples (Fig. 4B), demonstrating the high level of selectivity achieved by this method.

The statistical results shown in Table 1 also support this conclusion, implying good values for the root mean square error of prediction (RMSEP) and REP. The LODs obtained both in the absence and presence of interferences (2 and 4 ng mL⁻¹, respectively) are acceptable, taking into account that a very simple methodology is

applied to rather complex samples. It is necessary to recall that these limits have been calculated using the strict expressions recommended by IUPAC,³² as indicated above.

Real samples

The applicability of the proposed method was tested spiking with the analyte both water and fish samples found to be free from Hg(II) ion, and performing recovery studies. Figures 3C and 3D show three-dimensional plots of the EEFMs and the corresponding contour plots for samples of river water and tuna fish, both spiked with Hg²⁺. In comparing these figures with that of a typical validation sample (without spectral interferences), it is apparent that a zeroth-order (univariate) calibration could not be applied, unless a severe sample pretreatment for removing the contribution of matrix interferences is employed. However, pretreatment steps are not necessary or minimal when using second-order calibration, as in the present case.

The results provided by PARAFAC for the studied water samples (Table 2) are outstanding, suggesting that the method can overcome the problem of the presence of unexpected interferences (both metal ions and organic compounds) from environmental background matrices.

Table 1 summarizes the corresponding figures of merit obtained for these water samples. The obtained LOD is equal to that obtained for validation samples, indicating that the presence of additional constituents does not decrease the sensitivity of the method. Although the United State Environmental Protection Agency (US EPA)³⁶ has set a maximum contaminant level of Hg(II) in drinking water at 2 ng mL⁻¹, and a tolerance limit in surface water of 10 ng mL⁻¹,³⁷ higher concentrations can be detected (> 50 ng mL⁻¹) in industrial wastewaters.^{18,38} As a conclusion, the LOD calculated applying the present methodology is appropriate for determining Hg (II) ion in

environmental samples (surface waters and industrial wastewaters), as suggested by the US EPA, with the advantage that it was obtained applying a simple method with a minimal sample treatment, and without using organic solvents. The above described EJCR test was applied to these samples (data not shown) and the obtained result, with the theoretically expected values of slope = 1 and intercept = 0 included within the corresponding ellipse, corroborates the accuracy of the method.

The recovery results obtained for fish samples (Table 3), the corresponding EJCR test (data not shown) and the remaining statistical results (Table 1) were also very satisfactory. The US EPA has established a level of $0.55 \mu\text{g g}^{-1}$ of mercury in edible fish tissues.³⁹ On the other hand, the current allowable mercury level in commercial fish and fisheries products directed by the United State Food and Drug Administration (US FDA)⁴⁰ is $1.0 \mu\text{g g}^{-1}$. Therefore, the LOD value achieved through the proposed method ($\text{LOD} = 4 \times 10^{-3} \mu\text{g g}^{-1}$) is significantly lower than the above established levels, corroborating the usefulness of the method for the Hg(II) determination in this type of samples.

As indicated in the introduction, a significant number of reports describing the development of Hg(II) chemosensors using different strategies has been published. An original approach that should be mentioned is based on the fluorescence quenching effect of Hg(II) on CdS quantum dots-dendrimer nanocomposites. PARAFAC was employed for confirming the mechanism of action.⁴¹

In Table 4, important analytical characteristics of relevant chemosensors recently reported for the determination of Hg^{2+} are summarized and compared with the method here proposed. The reported LODs of the selected methods range from 0.4 to 200 ng mL^{-1} . It is important to take into account that these values were in general calculated as three times the standard deviation of the blank signal, yielding therefore

more favorable values, although they do not comply with the latest IUPAC recommendations.³²

The selectivity of the proposed method, which employs second-order calibration with the concomitant second-order advantage (see above), favorably compares with those using the traditional zeroth-order calibration, which could not overcome the problem of spectral interference from organic species. Finally, the fact that the experiments are carried out in aqueous solutions adds to the advantages of the proposed method.

Conclusions

A novel and environmentally friendly method for Hg(II) ion determination was described, using a fluorescence chemosensor based on a boron dipyrromethene tetraamine derivative (BODIPYTD) in combination with second-order multivariate calibration. Excitation-emission fluorescence matrices for the BODIPYTD-mercury complex were processed by PARAFAC, allowing the successful determination of the metal ion at levels required by regulatory agencies. The novelty of the proposed approach rests in the fact that it enabled determination of trace levels of the pollutant metal ion, even in the presence of potential organic interferences which display fluorescence signals in the same spectral range as the studied chemosensing mercury complex. The application of a chemometric tool makes it unnecessary to apply additional clean up steps for the removal of interfering compounds, saving experimental time and operator efforts, and avoiding the use of contaminating solvents. The obtained results suggest that the proposed approach is suitable for the analysis of mercury ion in environmental samples, favorably competing with current methods, without requiring expensive and sophisticated equipment and clean up procedures. The combined gains in

selectivity towards inorganic and organic interferents presage auspicious applications of chemosensors coupled to multivariate calibration in analytical laboratories.

Acknowledgements

The authors are grateful to the Universidad Nacional de Rosario, and Consejo Nacional de Investigaciones Científicas y Técnicas (CONICET), and Ministerio de Economía y Competitividad of Spain (Proyect CTQ2011-25388) and Gobierno de Extremadura (Proyect GR1003-FQM003), both co-financed by European FEDER funds, for financially supporting this work.

References

- 1 Website of the United State Environmental Protection Agency (U.S. EPA), Priority pollutants, <http://water.epa.gov/scitech/methods/cwa/pollutants.cfm>.
- 2 J. G. Dórea, *Sci. Total Environ.*, 2008, **400**, 93–114.
- 3 K. Leopold, M. Foulkes and P. Worsfold, *Anal. Chim. Acta*, 2010, **663**, 127–138.
- 4 V. Azevedo Lemos and L. Oliveira dos Santos, *Food Chem.*, 2014, **149**, 203–207.
- 5 Y. Gao, Z. Shi, Q. Zong, P. Wu, J. Su and R. Liu, *Anal. Chim. Acta*, 2014, **812**, 6–11.
- 6 J. Luo, S. Jiang, S. Qin, H. Wu, Y. Wang, J. Jiang and X. Liu, *Sens. Actuators B*, 2011, **160**, 1191–1197.
- 7 J. Zhang, Y. Zhou, W. Hu, L. Zhang, Q. Huang and T. Ma, *Sens. Actuators B*, 2013, **183**, 290–296.

- 8 D. Wu, Z. Wang, G. Wu and W. Huang, *Mater. Chem. Phys.*, 2012, **137**, 428–433.
- 9 D. Bohoyo Gil, M. I. Rodríguez–Cáceres, M. C. Hurtado–Sánchez and A. Muñoz de la Peña, *Appl. Spectrosc.*, 2010, **64**, 520–527.
- 10 V. A. Lozano, G. M. Escandar, M. C. Mahedero and A. Muñoz de la Peña, *Anal. Methods*, 2012, **4**, 2002–2008.
- 11 X. C. Fu, J. Wu, C. G. Xie, Y. Zhong and J. H. Liu, *Anal. Methods*, 2013, **5**, 2615–2622.
- 12 X. Zhang and Y. Y. Zhu, *Sens. Actuators B*, 2014, **202**, 609–614.
- 13 S. Atilgan, I. Kutuk and T. Ozdemir, *Tetrahedron Lett.*, 2010, **51**, 892–894.
- 14 D. Kim, K. Yamamoto and K. H. Ahn, *Tetrahedron*, 2012, **68**, 5279–5282.
- 15 T. K. Khan and M. Ravikanth, *Dyes Pigm.*, 2012, **95**, 89–95.
- 16 A. N. Kursunlu, P. Deveci and E. Guler, *J. Luminesc.*, 2013, **136**, 430–436.
- 17 J. Fan, X. Peng, S. Wang, X. Liu, H. Li and S. Sun, *J. Fluoresc.*, 2012, **22**, 945–951.
- 18 M. J. Culzoni, A. Muñoz de la Peña, A. Machuca, H. C. Goicoechea, R. Brasca and R. Babiano, *Talanta*, 2013, **117**, 288–296.
- 19 M. J. Culzoni, A. Muñoz de la Peña, A. Machuca, H. C. Goicoechea, R. Brasca and R. Babiano, *Anal. Methods*, 2013, **5**, 30–49.
- 20 F. Han, Y. Xu, D. Jiang, Y. Qin and H. Chen, *Anal. Biochem.*, 2013, **435**, 106–113.
- 21 A. Gałuszka, Z. Migaszewski and J. Namieśnik, *Trends Anal. Chem.*, 2013, **50**, 78–84.
- 22 K. S. Booksh and B. R. Kowalski, *Anal. Chem.*, 1994, **66**, 782A–791A.

- 23 G. M. Escandar, H. C. Goicoechea, A. Muñoz de la Peña and A. C. Olivieri, *Anal. Chim. Acta*, 2014, **806**, 8–26.
- 24 R. Bro, *Chemom. Intell. Lab. Syst.*, 1997, **38**, 149–171.
- 25 MATLAB R2011b, The MathWorks Inc., Natick, MA, USA.
- 26 <http://www.models.life.ku.dk/algorithms>.
- 27 A. C. Olivieri, H. L. Wu and R. Q. Yu, *Chemom. Intell. Lab. Syst.*, 2009, **96**, 246–251.
- 28 A. C. Olivieri and G. M. Escandar, *Practical three-way calibration*, Elsevier, Waltham, USA, 2014.
- 29 P. C. Damiani, I. Durán Merás, A. García Reiriz, A. Jiménez Jirón, A. Muñoz de la Peña and A. C. Olivieri, *Anal. Chem.*, 2007, **79**, 6949–6958.
- 30 R. Bro and H. A. L. Kiers, *J. Chemom.*, 2003, **17**, 274–286.
- 31 A. G. González, M. A. Herrador and A. G. Asuero, *Talanta*, 1999, **48**, 729–736.
- 32 A. C. Olivieri, *Chem. Rev.*, 2014, **114**, 5358–5378.
- 33 X. Zhao, X. Hu and H. M. Hwang, *Chemosphere*, 2006, **63**, 1116–1123.
- 34 Y. S. Al-Degs, R. A. El-Halawa, and S. S. Abu-Alrub, *Chem. Eng. J.*, 2012, **191**, 185–194.
- 35 S. Chiron, C. Minero and D. Vione, *Environ. Sci. Technol.*, 2006, **40**, 5977–5983.
- 36 Website of the United State Environmental Protection Agency (U.S. EPA), Water: historical archive of drinking water contaminant fact sheets, <http://water.epa.gov/drink/contaminants/basicinformation/mercury.cfm>.
- 37 M. K. Hafshejani, A. Vahdati, M. Vahdati, A.B. Kheradmand, M. Sattari, A. Arad and S. Choopani, *Life Sci. J.*, 2012, **9**, 1846–1848.

- 38 M. G. Afshar, M. Soleimani and M. Bazrpach, *World Acad. Sci. Eng. Techn.*, 2011, **5**, 283–284.
- 39 US-EPA, Regulatory impact analysis of the clean air Mercury rule: EPA-452/R-05-003, 2005.
- 40 J. M. Hightower and D. L Brown, *Environ. Health*, 2011, **10**, doi:10.1186/1476-069X-10-90.
- 41 B. B. Campos, M. Algarra, B. Alonso, C. M. Casado and J.C.G. Esteves da Silva, *Analyst*, 2009, **134**, 2447–2452.

Table 1 Statistical results for Hg(II) in synthetic and real samples

	Validation ^a	Test ^b	Water ^c		Fish ^d
LOD ^e (ng mL ⁻¹)	2	4	2	LOD ^e (μg g ⁻¹)	4×10 ⁻³
LOQ ^f (ng mL ⁻¹)	6	12	6	LOQ ^f (μg g ⁻¹)	1.2×10 ⁻²
RMSEP ^g (ng mL ⁻¹)	2	2	2	RMSEP ^g (μg g ⁻¹)	2×10 ⁻³
REP ^h (%)	3	5	3	REP ^h (%)	4
(R ²) ⁱ	0.9989	0.9928	0.9961	(R ²) ⁱ	0.9932

^a Twelve samples. ^b Twelve samples containing riboflavin, erythrosine and acridine as interferents. ^c Three different natural waters evaluated at three Hg(II) levels each.

^d Three different muscle tissue of fish (tuna and mackerel) samples evaluated at two Hg(II) levels each. ^e LOD, limit of detection calculated according to ref. 32. ^f LOQ, limit of quantitation calculated as LOD×(10/3.3). ^g RMSEP, root-mean-square error of prediction. ^h REP, relative error of prediction. ⁱ R², correlation coefficient.

Table 2 Recovery study of Hg(II) for spiked water samples using PARAFAC

Sample	Taken (ng mL ⁻¹)	Found (ng mL ⁻¹) ^a	Recovery (%)
River water	10.0	10 (2)	100
(Paraná River)	20.0	21 (3)	105
	30.0	34 (1)	112
Underground water	10.0	10 (1)	100
(Venado Tuerto City)	20.0	20 (1)	100
	30.0	31 (1)	103
Underground water	10.0	10 (1)	100
(Santa Rosa City)	20.0	19 (3)	95
	30.0	32 (2)	107

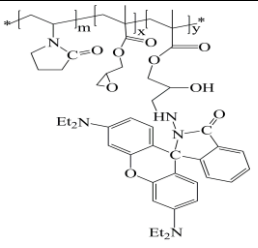
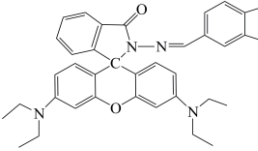
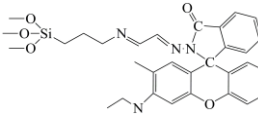
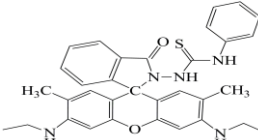
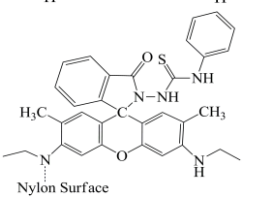
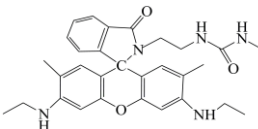
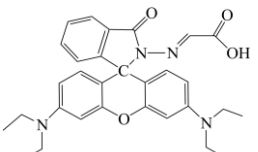
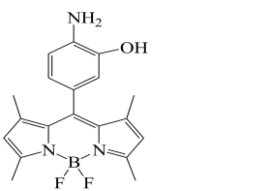
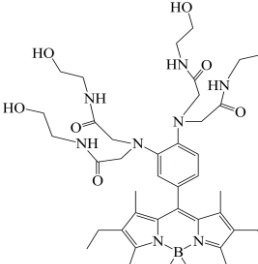
^a Mean of two determinations. Standard deviations between parentheses.

Table 3 Recovery study of Hg(II) for spiked fish samples using PARAFAC

Sample ^a	Taken ($\mu\text{g g}^{-1}$)	Found ($\mu\text{g g}^{-1}$) ^b	Recovery (%)
Tuna #1	0.12	0.11 (0.01)	93
	0.30	0.36 (0.02)	120
Tuna #2	0.12	0.10 (0.01)	83
	0.30	0.27 (0.01)	90
Mackerel	0.12	0.11 (0.01)	92
	0.30	0.31 (0.01)	103

^a Tuna #1 and #2 refer to two different specimens of tuna fish. ^b Mean of two determinations. Standard deviations between parentheses.

Table 4 Analytical performance of selected chemosensors recently reported for the determination of Hg(II) ion

Sensor ^a	Chemical structure	Reaction medium	Calibration data order	LOD ^b	Sample	Ref.
RD1		Aqueos	Zeroth-	10	Water	6
RD2		Aqueos	Zeroth-	2.4	Water	7
RD3		Aqueos	Zeroth-	2	Water	8
RD4		Organic	Zeroth-	0.7 ^d	Water, fish	9
RD5		Aqueos	Zeroth-	0.4	Water	10
RD6		Organic	Zeroth-	20	Water	11
RD7		Aqueos	Zeroth-	200	Water	12
BD1		Organic	Zeroth-	≤ 2	Water	17
BD2		Aqueos	Zeroth-	5.5	Water	18
BD3	Idem BD2	Aqueos	Second- ^c	2 ^d	Water, fish	This work

^a RD = rhodamine derivative, BD = BODIPY derivative. ^b LODs are given in ng mL⁻¹. ^c In the presence of organic interferents (see text). ^d LOD refers to water samples.

Figure Captions

Fig. 1 Structure of BODIPYTD: 4,4-difluoro-8-(aryl)-1,3,5,7-tetramethyl-2,6-diethyl-4-bora-3a,4a-diaza-*s*-indacene, where aryl = 3,4-(bis((bis(2-(2-hydroxyethyl)amino)-2-oxoethyl)amino))phenyl.

Fig. 2 (A) Excitation and emission fluorescence spectra for the free BODIPY derivative (dashed red lines) and for the BODIPY derivative in the presence of 20, 40, 60, 80 and 100 ng mL⁻¹ Hg(II) ion (solid lines). (B) Normalized excitation and emission fluorescence spectra for the free BODIPY derivative (dashed red lines) and for the BODIPY derivative-Hg²⁺ complex (black lines). (C) Normalized excitation and emission fluorescence spectra for the BODIPY-Hg²⁺ complex (black lines), riboflavin (green lines), erythrosine (cyan lines) and acridine (pink lines) under the applied experimental conditions (pH = 7.5).

Fig. 3 Three-dimensional plots and the corresponding contour plots of excitation-emission matrices for (A) a validation sample containing 21.0 ng mL⁻¹ Hg(II), (B) a test sample containing 18.0 ng mL⁻¹ Hg(II), 100 ng mL⁻¹ riboflavin, 100 ng mL⁻¹ erythrosine and 250 ng mL⁻¹ acridine, (C) a spiked river sample ($C_{\text{Hg(II)}} = 16.2 \text{ ng mL}^{-1}$), and (D) a spiked tuna fish sample after nitric acid treatment ($C_{\text{Hg(II)}} = 15 \text{ ng mL}^{-1}$). In all cases $C_{\text{BODIPYTD}} = 2.00 \times 10^{-5} \text{ mol L}^{-1}$.

Fig. 4 Plots of PARAFAC Hg(II) predicted concentrations as a function of the nominal values for validation samples (A), and for samples with interferences (test samples) (B). In (A) and (B) the solid lines are the perfect fits. (C) Elliptical joint regions (at 95 % confidence level) for slopes and intercepts of the regression for validation (blue line) and for test (red line) samples. The black circle marks the theoretical (intercept = 0, slope = 1) point.

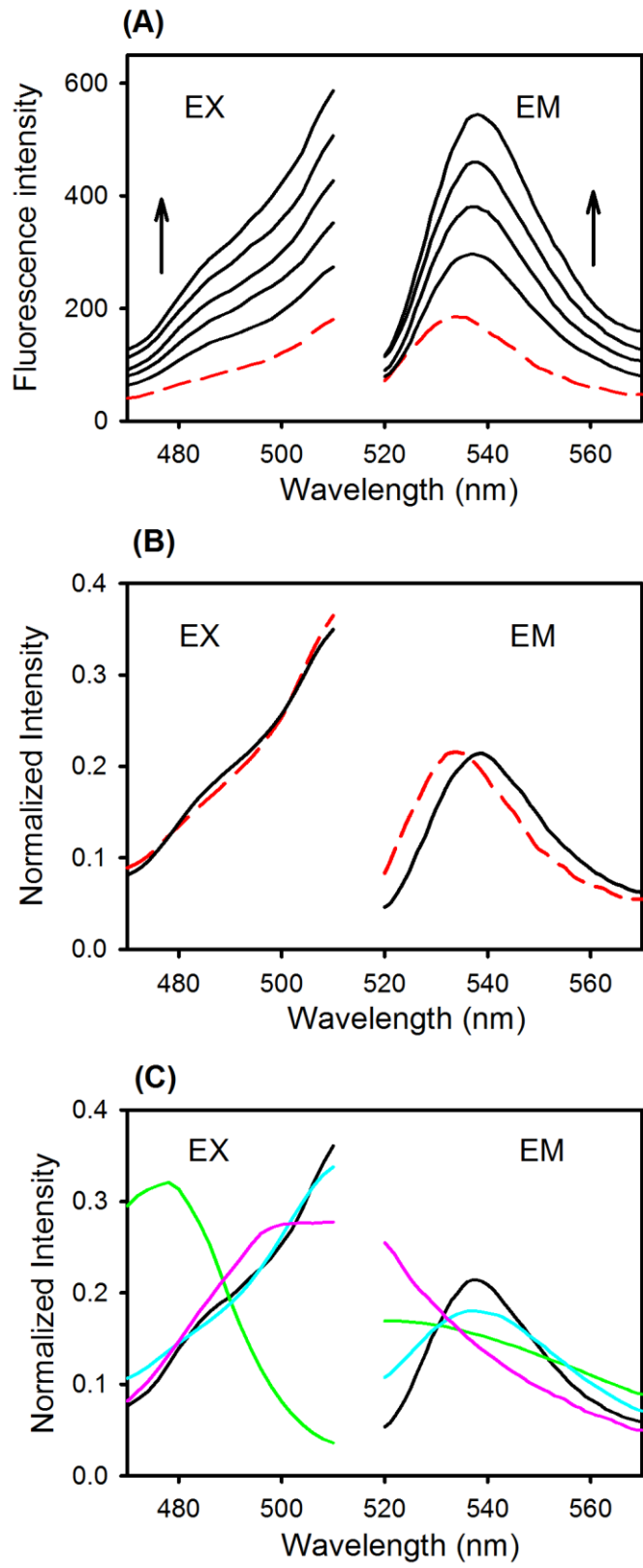


FIGURE 2

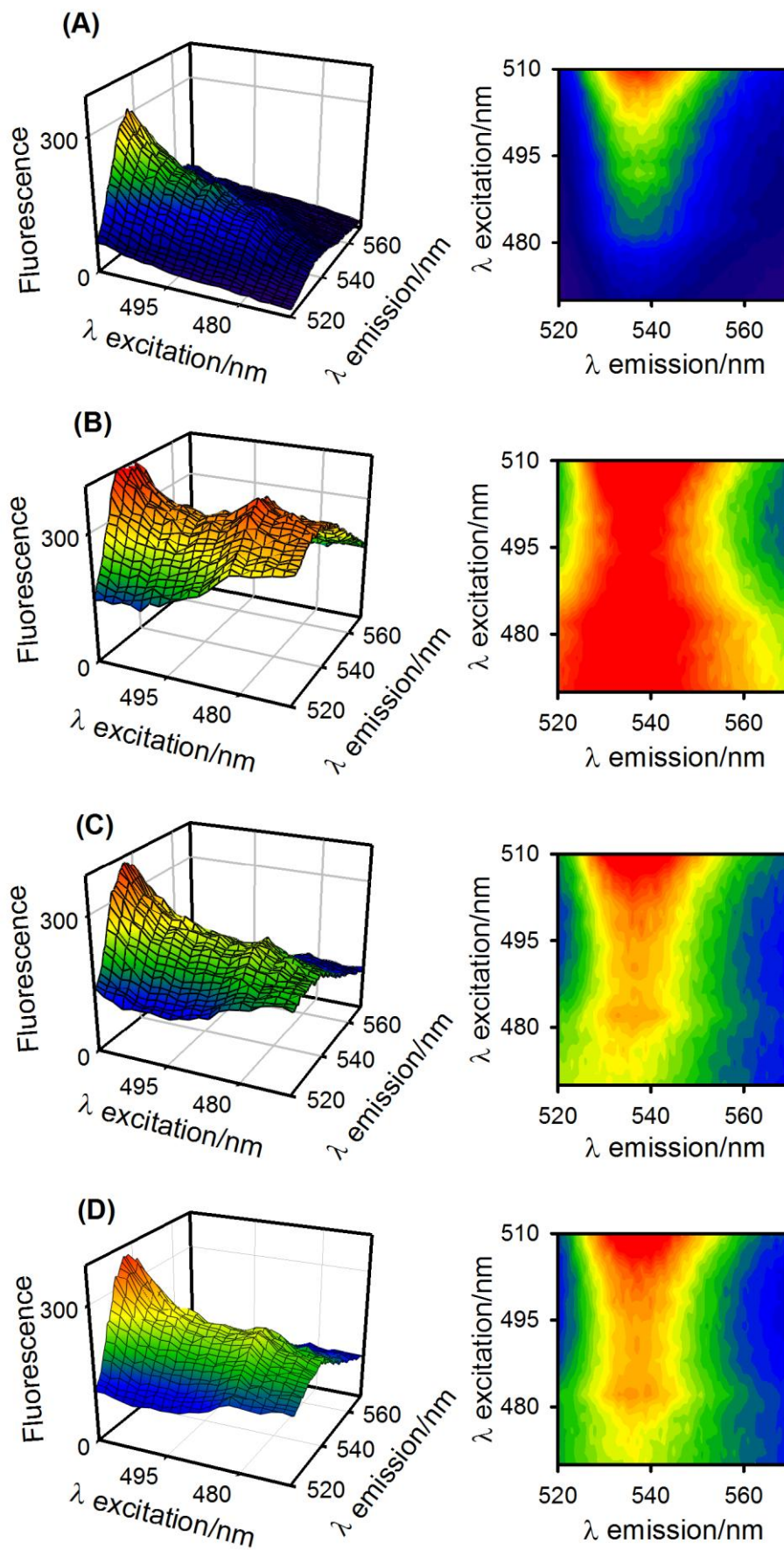


FIGURE 3

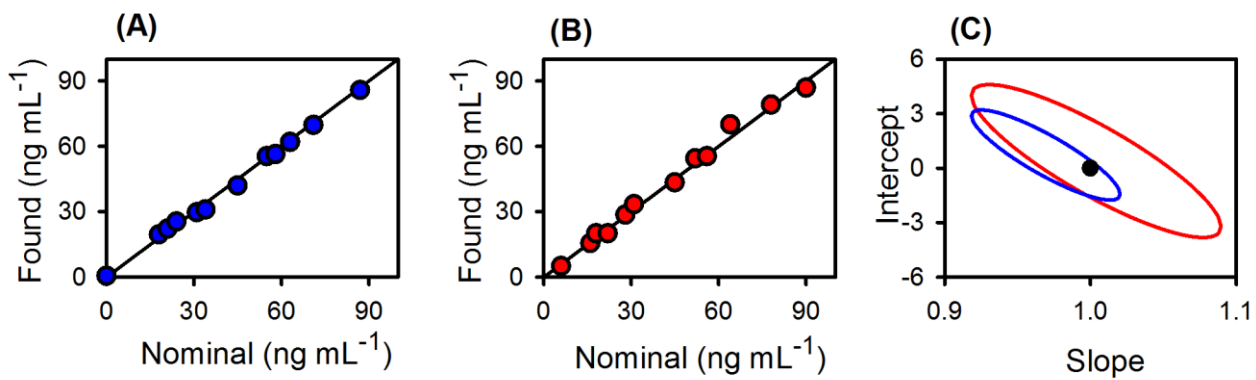


FIGURE 4